Vol. 33 (2002) *ACTA PHYSICA POLONICA B* No 7

AZIMUTHAL ANISOTROPIES IN NUCLEAR FRAGMENTATION

A. Dąbrowska, M. Szarska, A. Trzupek, W. Wolter and B. Wosiek

Henryk Niewodniczański Institute of Nuclear Physics
Radzikowskiego 152, 31-342 Kraków, Poland

(Received April 17, 2002)

The directed and elliptic flow of fragments emitted from the excited projectile nuclei has been observed for 158 A GeV Pb collisions with the lead and plastic targets. For comparison the flow analysis has been performed for 10.6 A GeV Au collisions with the emulsion target. The strong directed flow of heaviest fragments is found. Light fragments exhibit directed flow opposite to that of heavy fragments. The elliptic flow for all multiply charged fragments is positive and increases with the charge of the fragment. The observed flow patterns in the fragmentation of the projectile nucleus are practically independent of the mass of the target nucleus and the collision energy. Emission of fragments in nuclear multifragmentation shows similar, although weaker, flow effects.

PACS numbers: 25.75.+r, 29.40.Rg

1. Introduction

The study of azimuthal anisotropy of charged particle emission from high energy nuclear collisions has attracted a lot of interest from both experimentalists and theorists. Such study should reveal whether the produced matter behaves collectively due to the compression effects existing in the initial stage of the collision. The collective flow observables may carry information about the degree of equilibration attained during the system evolution, on the nuclear equation of state and should reflect the spatial anisotropy of the collision zone in non-central nucleus–nucleus collisions [1–4]

Data analysis at low and intermediate energies concentrated on the determination of the direction of longitudinal flow. At ultra-relativistic energies this flow direction coincides with the collision axis and, therefore, the search for the collective effects should be performed in the transverse direction, in the plane orthogonal to the collision axis. Such studies have been performed for nucleus–nucleus data from AGS [5, 6] and SPS [7, 8] accelerators, and recently also for Au+Au collisions at RHIC energy [9–11]. They concentrated on the search for azimuthal anisotropies in the emission of produced particles.

The analysis presented in this paper is focused on the search for collective flow effects in the emission of fragments from the excited Pb projectile nucleus in Pb interactions with heavy and light nuclear targets at the energy of 158 A GeV. The data will be compared to the results obtained at lower energy, for Au collisions with the emulsion target at 10.6 A GeV.

2. Experimental data

The data were obtained from the EMU13 emulsion chambers exposed to the Pb beam from SPS at CERN. Emulsion chambers, used in the EMU13 experiment, were composed of lead target foils and thin emulsion plates interleaved with spacers of varied thicknesses. Details of emulsion chambers used in this experiment as well as irradiation conditions can be found elsewhere [12–14]. A unique set-up of the emulsion chambers enabled precise measurements of emission angles and charges of all forward going particles.

Scanning for minimum bias Pb+Pb and Pb+($C_5H_4O_2$) (plastic base of emulsion plates) interactions was done under the microscope in the upper part of the emulsion chambers. Details of scanning for Pb interactions can be found in [12]. This scanning was inefficient in finding very peripheral collision events, in which a single nuclear fragment is emitted whose charge is not very different from that of the primary Pb nucleus. In order to avoid this scanning bias, the present analysis is restricted to the events characterized by the charge change $\Delta Z = Z_p - Z_1 > 14$, for which our scanning was 100% efficient (Z_p denotes the charge of the projectile nucleus and Z_1 is the charge of the heaviest fragment in an event). The samples of such selected events will be referred to as semi-inclusive samples. The above ΔZ criterion was fulfilled by 435 Pb+Pb interactions and 484 Pb+PL[1] collisions. For Pb+PL collisions the selected sample corresponds to 56% of the total charge changing nuclear cross-section. The sample of semi-inclusive Pb+Pb interactions represents 64% of the total charge changing nuclear cross-section and includes the events of both electromagnetic and nuclear origin [15].

The flow analysis concerns particles emitted in the projectile fragmentation region which is defined by the cut in the polar emission angle, $\theta \leq 3.8$ mrad ($\eta = -\ln\tan\theta/2 \geq 6.26 = \eta_{\rm frag}$). In this forward cone multiply charged fragments are characterized by their charges, Z. All singly charged particles contained in this cone are referred to as singly charged spectators.

[1] In this paper we will use an abbreviation (PL) to denote the PLastic ($C_5H_4O_2$) target.

We also extend the analysis to larger emission angles, $\eta_{\rm frag} - 1 \leq \eta < \eta_{\rm frag}$, where singly charged relativistic particles will be called "pions", although they may represent a mixture of produced pions and participant protons.

In the plane (x, y) perpendicular to the collision axis (z), the track coordinate measurements were made with the precision of about 0.2 μm over a distance of about 20 cm along the z-axis. Consequently, the accuracy of the measured track opening angles (θ, φ) is mainly determined by the uncertainty in the event axis, *i.e.* the direction of the primary nucleus. For every event, the beam position in the plane perpendicular to the collision axis was defined as charge weighted center of the track coordinates. Fragments with $Z \geq 10$ were used to calculate the charge weighted center. For events with the charge of the heaviest fragment smaller than 10, the center was calculated from all multiply charged fragments. All multiply and singly charged fragments were used for evaluating the beam center in events with at most single $Z = 2$ fragment.

The data for gold nuclei collisions with the EMulsion (EM) target (Au+EM) at 10.6 A GeV from the E868 experiment at AGS [16–18], used for comparison, were selected by the same criterion $\Delta Z > 14$. The selected sample corresponds to 75% of most central events of nuclear origin. The fragmentation region is defined by the $\eta_{\rm frag} = 4.4$ [18]. The same procedure, as described above, was used to determine the (x, y) position of the beam axis.

3. Analysis procedure

The most commonly used method of the analysis of azimuthal anisotropies is based on the Fourier expansion of the distribution of the particle azimuthal angle, φ

$$E\frac{d^3N}{dp^3} = \frac{1}{2\pi}\frac{d^2N}{p_{\rm T}dp_{\rm T}dy}\left[1 + \sum_{n=1}^{\infty} 2v_n \cos[n(\varphi - \psi_{\rm R})]\right] , \qquad (1)$$

where $\psi_{\rm R}$ is the azimuthal angle of the reaction plane, defined by the impact parameter and the beam axis. The first term in the square brackets represents the isotropic radial flow. The Fourier coefficients, v_n, measure the anisotropy of the distribution. The first coefficient, $v_1 = \langle\cos(\varphi - \psi_{\rm R})\rangle$ is called directed flow, the second one, $v_2 = \langle\cos[2(\varphi - \psi_{\rm R})]\rangle$ is referred to as the elliptic flow. In this analysis the flow coefficients, integrated over the particle transverse momenta, are studied in the projectile fragmentation region.

From Eq. (1) it is evident that the most crucial part of any flow study is the ability to measure the reaction plane on an event-by-event basis. In this analysis, we follow the procedure proposed by Poskanzer and Voloshin [19], which uses the anisotropic flow itself to determine the event plane angle as the experimental estimate of the reaction plane angle. For every event, both first harmonic ψ_1, and second harmonic ψ_2, were determined by

$$\psi_n = \frac{1}{n}\tan^{-1}\left(\frac{\sum w_i(\varphi_i)\sin(n\varphi_i)}{\sum w_i(\varphi_i)\cos(n\varphi_i)}\right), \tag{2}$$

where $n = 1, 2$, the sums go over all particles contained in the projectile fragmentation region ($\eta \geq \eta_{\rm frag}$) and φ_i is the measured (laboratory) azimuthal angle of the i-th particle. Weights, w_i, were used to remove the correlations due to the acceptance effects and/or other measurement related biases. For this analysis we use weights determined for each φ bin as the inverse of the charged weighted content of the i-th bin summed over all events. It should be noted that our results are not very sensitive to the particular choice of weights (even with setting all w_i to 1), which is understandable since the measured $dN/d\varphi$ distributions are practically uniform. However, with this weighting, the event plane azimuthal angle distributions were flat within the statistics. For illustration see Fig. 1(a) and (b) where event plane angle distributions are shown for the semi-inclusive sample of Pb+Pb collisions.

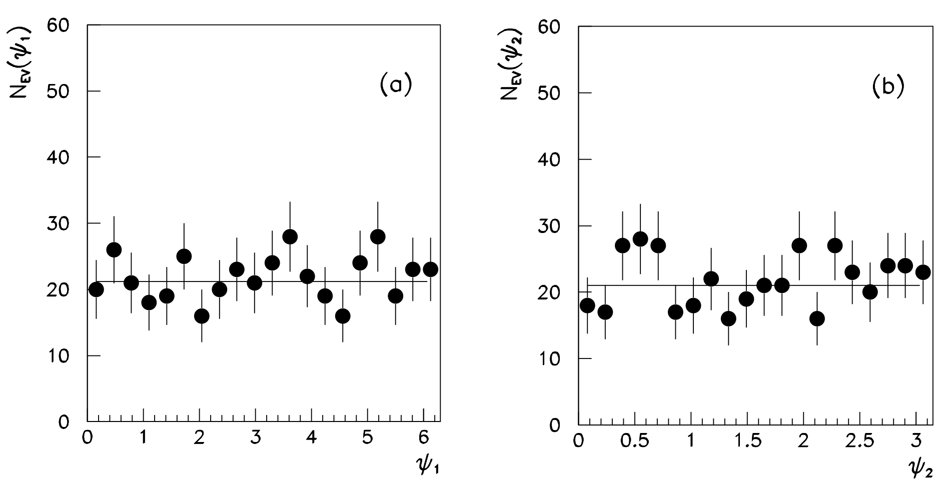

Fig. 1. Distributions of the first ψ_1 (a) and second ψ_2 (b) harmonic of the event plane angle for Pb+Pb collisions at 158 A GeV. Lines show the 0-th order polynomial fits to the data.

The experimental approximation of the true reaction plane angle by the measured event plane angles Eq. (2) suffers from the limited resolution due to the the finite number of detected particles [19,20]. Therefore, the resolution corrections, r_n, should be applied. They can be obtained from the correlation between event plane angles determined for the two equal multiplicity sub-events

$$r_n = \sqrt{2\langle\cos[n(\psi_n^a - \psi_n^b)]\rangle}\,, \tag{3}$$

where ψ_n^a and ψ_n^b denote the event plane angles calculated from Eq. (2) for the two sub-events: a and b. A factor of 2 under the square root accounts for the difference between event and sub-event multiplicities. The sub-events have been chosen by randomly dividing all (charge weighted) particles contained in the fragmentation region into two independent sets of particles. The determined resolution correction factors are close to unity, indicating that the sub-events are strongly correlated. This is not surprising in the study including multiply charged fragments, since the presence of a single heavy projectile fragment is sufficient to precisely determine the reaction plane.

As a final step, the flow coefficients are calculated as $v_1 = \langle\overline{\cos(\varphi - \psi_1)}\rangle / r_1$ and $v_2 = \langle\overline{\cos[2(\varphi - \psi_2)]}\rangle / r_2$, where the brackets $\langle\,\rangle$ denote averaging over all events, and bars refer to the averaging over all particles in a given event. The event quantities were obtained as charge weighted averages. In order to remove the auto-correlation effect, each particle in a given event was correlated with the event plane angle determined from all the other particles.

4. Results for semi-inclusive collisions

The flow coefficients, v_n, were measured separately for the following particle types: singly charged fragments ($Z = 1$), helium fragments ($Z = 2$), light fragments ($3 \leq Z \leq 6$), medium-size fragments ($7 \leq Z \leq 29$) and heavy fragments ($Z \geq 30$). In addition, the flow coefficients were also calculated for "pions", *i.e.* singly charged particles emitted in the pseudo-rapidity region $\eta_{\mathrm{frag}} - 1 \leq \eta < \eta_{\mathrm{frag}}$. Table I lists v_1 values for different particles for Pb+Pb and Pb+PL collisions at 158 A GeV. For comparison the results obtained from the analysis of Au+EM collisions at 10.6 A GeV were also included.

The corresponding v_2 coefficients are quoted in Table II. It can be seen that for pions the both flow coefficients are very small. This indicates that these particles show a flow effects smaller than about 1% which is the limit of our sensitivity, mainly due to the low event statistics. The effects observed for fragmentation products are discussed below.

TABLE I

Directed flow coefficients, v_1, calculated for different particle species for semi-inclusive Pb+Pb and Pb+PL collisions at $158A$ GeV, and Au+EM collisions at $10.6A$ GeV.

Particle	Pb+Pb 158 A GeV	Pb+PL 158 A GeV	Au+EM 10.6 A GeV
Spectators $Z=1$	0.012 ± 0.011	0.006 ± 0.008	0.024 ± 0.008
Helium $Z=2$	0.036 ± 0.019	0.026 ± 0.014	0.035 ± 0.011
Fragments $3 \leq Z \leq 6$	$-.245 \pm 0.040$	$-.257 \pm 0.033$	$-.165 \pm 0.024$
Fragments $6 \leq Z \leq 29$	0.029 ± 0.046	$-.027 \pm 0.042$	0.182 ± 0.028
Fragments $Z \geq 30$	0.553 ± 0.051	0.614 ± 0.033	0.589 ± 0.027
Fragments $Z \geq 3$	0.305 ± 0.023	0.335 ± 0.019	0.335 ± 0.014
Pions $Z=1$	0.014 ± 0.011	0.006 ± 0.010	0.032 ± 0.008

TABLE II

Elliptic flow coefficients, v_2, calculated for different particle species for semi-inclusive Pb+Pb and Pb+PL collisions at 158 A GeV, and Au+EM collisions at 10.6 A GeV.

Particle	Pb+Pb 158 A GeV	Pb+PL 158 A GeV	Au+EM 10.6 A GeV
Spectators $Z=1$	0.012 ± 0.009	$-.009 \pm 0.006$	0.004 ± 0.007
Helium $Z=2$	0.052 ± 0.018	0.037 ± 0.014	0.083 ± 0.011
Fragments $3 \leq Z \leq 6$	0.334 ± 0.036	0.322 ± 0.028	0.314 ± 0.020
Fragments $6 \leq Z \leq 29$	0.621 ± 0.030	0.593 ± 0.025	0.585 ± 0.017
Fragments $Z \geq 30$	0.736 ± 0.034	0.664 ± 0.025	0.651 ± 0.019
Fragments $Z \geq 3$	0.579 ± 0.024	0.544 ± 0.018	0.519 ± 0.013
Pions $Z=1$	0.009 ± 0.010	0.017 ± 0.010	$-.008 \pm 0.007$

The experimental azimuthal angle distributions measured with respect to the event plane angle ψ_1 (ψ_2) are shown in Fig. 2 (Fig. 3) for $Z = 1$, $Z = 2$, and $3 \leq Z \leq 6$ fragments for the three analyzed data samples. It can be seen from Fig. 2 that for singly charged spectators the effect of the directed flow is negligible. It starts to build up for helium fragments, where a small indication of the positive directed flow can be seen, leading to the slight excess in the yield of particles at $\varphi - \psi_1 = 0, 2\pi$.

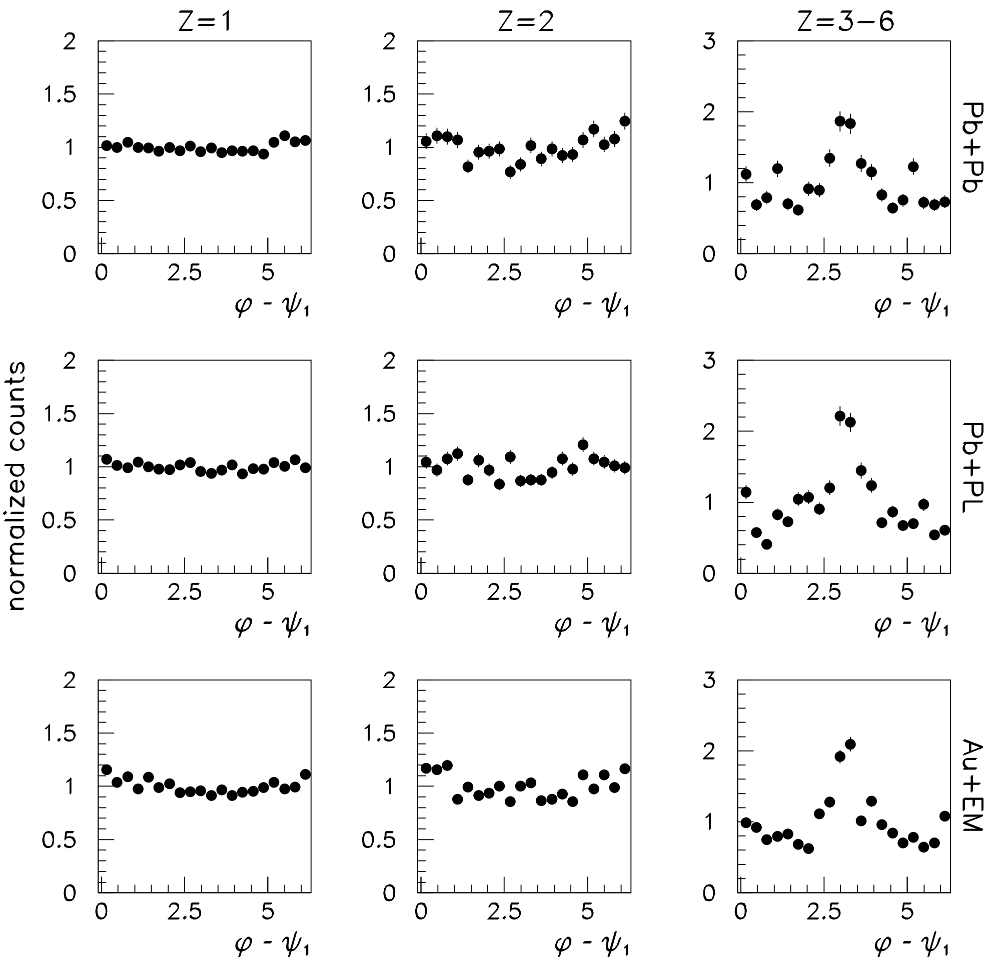

Fig. 2. Azimuthal angle distributions with respect to the event plane angle ψ_1 for fragments with $Z = 1$ (left panel), $Z = 2$ (middle panel) and $Z = 3 - 6$ (right panel). Top, middle and bottom panels correspond to the different data samples as indicated on the right side of the figure. The distributions have been normalized to an average value per bin of one.

Interestingly, for light fragments ($3 \leq Z \leq 6$) this tendency is reversed, and the anti-flow effect (preferential emission at π) is clearly seen. As can be seen from Table I, the still heavier fragments again exhibit the positive directed flow. This anti-flow signal observed for light fragments can be due to anti-correlations induced by the momentum conservation. Indeed, in about 85% of events with light fragments there is an accompanying significantly heavier fragment.

The azimuthal angle distributions measured with respect to ψ_2 (see Fig. 3) show a negligible asymmetry for singly charged fragments. For helium fragments the in-plane emission ($v_2 > 0$) starts to show up, and for still heavier fragments the in-plane particle emission is very clearly seen. The positive v_2 values mean that the ellipse is aligned with the reaction plane.

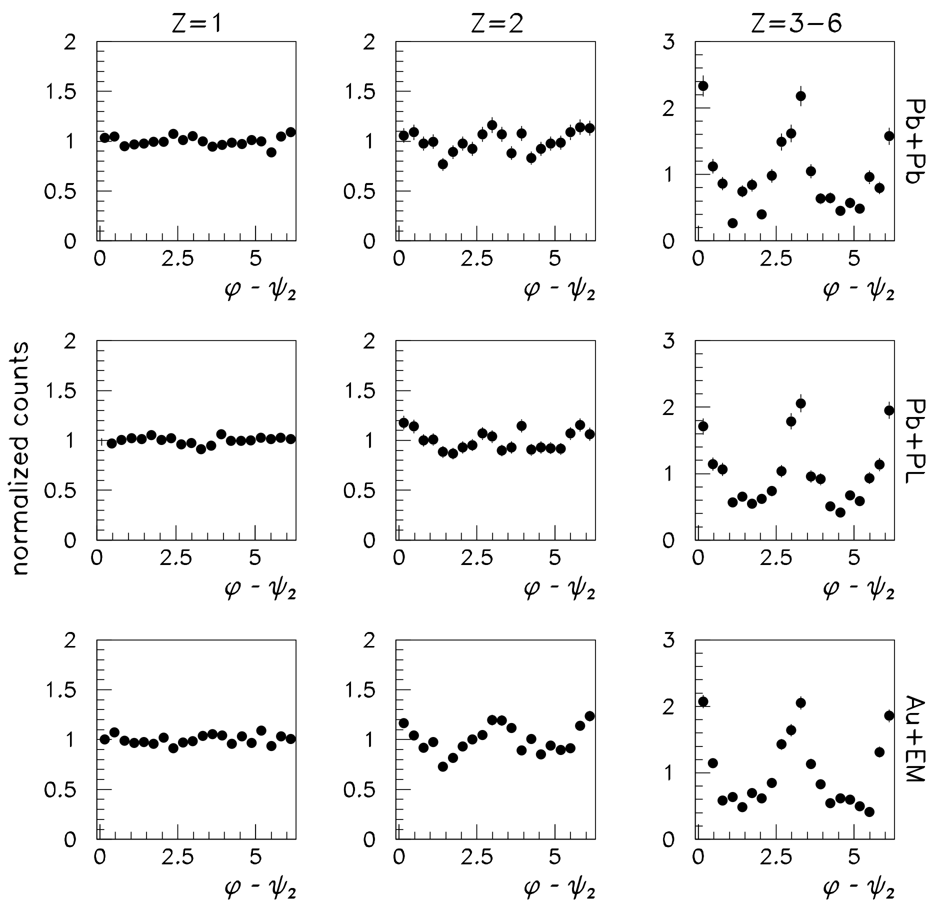

Fig. 3. The same as in Fig. 2 but for azimuthal angle distributions measured with respect to the second harmonic of the event plane angle, ψ_2.

The dependence of the flow coefficients on the fragment charge is shown in Fig. 4. One can see that both v_1 and v_2 coefficients weakly depend on the collision system. This observation of the similar flow patterns for fragments emitted from the excited projectile nucleus in different collision systems, suggests the common underlying mechanism responsible for the fragment emission. The observed directed and elliptic flow effects are negligible for $Z \leq 2$ fragments. For all data samples, the light fragments show systematically the anti-flow effect in v_1. The elliptic flow signal increases with the charge of the fragments, and the heaviest fragments show the considerable in-plane anisotropy of the order of 70%.

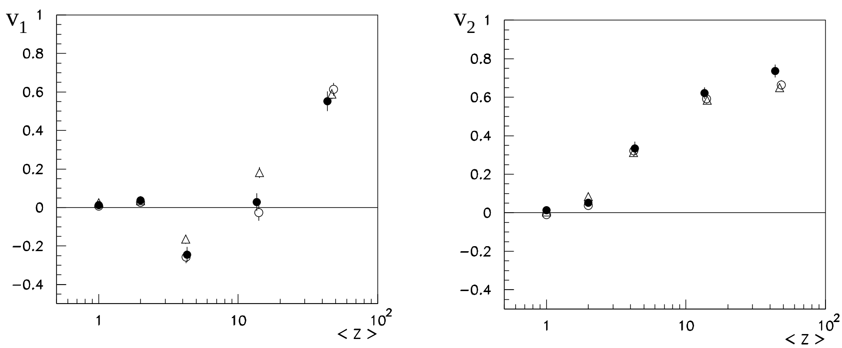

Fig. 4. Directed (v_1) and elliptic (v_2) flow coefficients as a function of the charge of the fragment for Pb+Pb (full circles), Pb+PL (open circles) and Au+EM (triangles) semi-inclusive collisions.

5. Flow analysis for nuclear multifragmentation

We have also performed the Fourier analysis of the azimuthal angle distributions of fragments emitted in the process of nuclear multifragmentation. This process is characterized by the emission of at least three relatively light fragments ($Z \leq 30$) and has been intensively studied due to its possible association with the liquid–gas phase transition. The detail description of the selection of multifragmentation events can be found in [21]. In [21] we have shown that the properties of multifragmentation events, such as multiplicity and charge distributions of fragments, do not depend on the mass of the target nucleus for Pb interactions at 158 A GeV, and also do not differ from those measured for multifragmentation of gold nuclei in Au+EM collisions at 10.6 A GeV. It is interesting to see whether the same universality is observed in a more detailed study of the azimuthal anisotropies. So, the same analysis procedure was applied to the selected multifragmentation events. In Fig. 5 the dependence of the flow coefficients on the fragment charge is shown for the three data sets. For multifragmentation of Pb projectile in

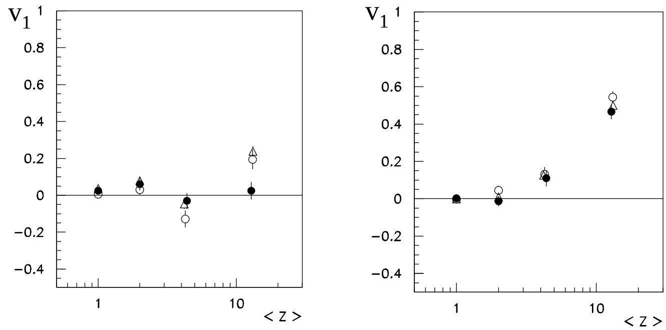

Fig. 5. The same as in Fig. 4, but for the samples of selected multifragmentation events.

Pb+Pb collisions the directed flow effect is very small, even for the heaviest analyzed fragments. For these heaviest fragments, the stronger signal is observed for Pb+PL and Au+EM data samples. The elliptic flow signal increases with the fragment charge and shows a very weak dependence on the projectile energy. The comparison to the results obtained from the study of semi-inclusive data samples is shown in Fig. 6. For Pb(158 A GeV)+Pb

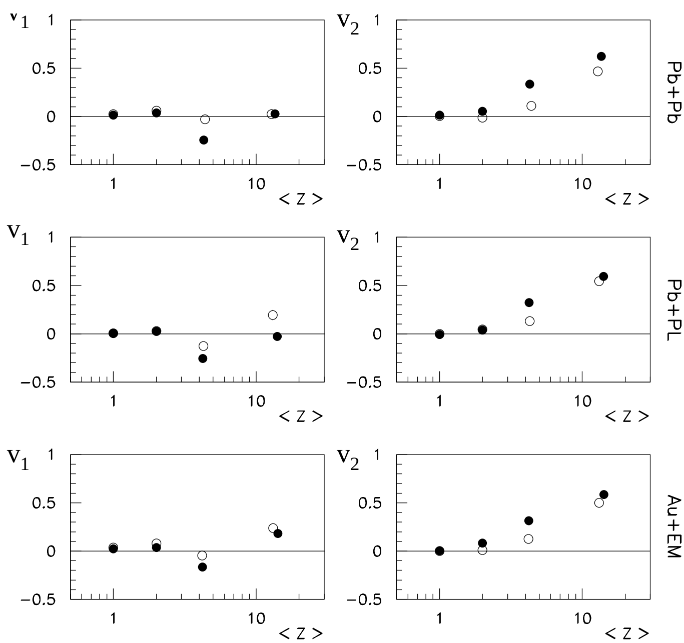

Fig. 6. Comparison of the directed (v_1) and elliptic (v_2) flow coefficients measured in semi-inclusive (full circles) and multifragmentation (open circles) events. From top to bottom, the results for different collision systems are shown as indicated on the right side of the figure.

and Au(10.6 A GeV)+EM collisions the elliptic flow effects are systematically weaker in multifragmentation as compared to semi-inclusive data sets. This observation is not so evident for the Pb(158 A GeV)+PL collisions.

6. Summary and conclusions

We have presented the data on azimuthal anisotropies in the fragment emission from the excited projectile nuclei in Pb+Pb and Pb+PL collisions at 158 A GeV and for Au collisions with the emulsion target at 10.6 A GeV. The analysis has been performed for semi-inclusive data sets as well as for selected multifragmentation events.

It should be noted that electronic experiments have no sensitivity to perform the flow measurements at the very small forward angles. The only high energy data on azimuthal anisotropies in the emission of projectile fragments were shown in [22, 23], where strong flow effects in nuclear fragmentation were reported. The direct comparison to the results presented in [22, 23] is not possible since they were based on the different event selections and the different analysis method.

The main advantage of the analysis of flow effects for nuclear fragments is that the measurements of emission angles and charges of multiply charged fragments ensure a rather precise experimental determination of the reaction plane. This high accuracy is of vital importance for the analysis relied on the Fourier decomposition of the azimuthal angle distributions.

A strong directed flow signal is observed in the emission of heaviest fragments in semi-inclusive data samples. This signal was found to be independent of the mass of the target nucleus and the energy of the fragmenting projectile. For very light fragments we observe a directed anti-flow effect probably due to the momentum conservation. The elliptic flow signal increases with increasing charge of the fragment, reaching the value of about 70% for the heaviest fragments. The observed elliptic flow patterns are independent of the size of the system and primary energy. For all multiply charged fragments the in-plane elliptic flow is measured, indicating that at these high energies the flow of the spectator matter should not prohibit an in-plane flow of the produced particles. In fact the results on the elliptic flow of produced particles are consistent with the positive ($v_2 > 0$) flow signal in ultra-relativistic nuclear collisions.

Similar effects were observed for the selected multifragmentation events, although the magnitude of the elliptic flow is systematically smaller as compared to the semi-inclusive collisions. The presented results show evidence for a universal pattern of the fragment emission in fragmentation processes at ultra-relativistic energies.

This work was partially supported by the Polish State Committee for Scientific Research (KBN) grant no. 2P03B05417.

REFERENCES

[1] H. Sorge, *Phys. Rev. Lett.* **82**, 2048 (1999).
[2] W. Reisdorf, H.G. Ritter, *Ann. Rev. Nucl. Part. Sci.* **47**, 663 (1997).
[3] P. Kolb, J. Sollfrank, U. Heinz, *Phys. Lett.* **B459**, 667 (1999).
[4] D. Teaney, E.V. Shuryak, *Phys. Rev. Lett.* **83**, 4951 (1999).
[5] C. Pinkenburg *et al.*, E895 Collaboration, *Phys. Rev. Lett.* **83**, 1295 (1999).
[6] J. Barrette *et al.*, E877 Collaboration, *Phys. Rev.* **C56**, 3254 (1997).
[7] H. Appelshauser *et al.*, NA49 Collaboration, *Phys. Rev. Lett.* **80**, 4136 (1998).
[8] M.M. Aggarwal *et al.*, WA98 Collaboration, *Nucl. Phys.* **A638**, 459 (1998).
[9] K.H. Ackermann *et al.*, STAR Collaboration, *Phys. Rev. Lett.* **86**, 402 (2001).
[10] C. Adler *et al.*, STAR Collaboration, *Phys. Rev. Lett.* **87**, 182301 (2001).
[11] B.B. Back *et al.*, PHOBOS Collaboration, *Nucl. Phys.* **A698**, 564 (2002).
[12] M.L. Cherry *et al., Acta Phys. Pol.* **B29**, 2155 (1998).
[13] P. Deines-Jones *et al., Phys. Rev.* **C53**, 3044 (1996).
[14] P. Deines-Jones *et al., Phys. Rev.* **C62**, 014903 (2000).
[15] A. Dąbrowska *et al.*, to be published.
[16] M.L. Cherry *et al., Phys. Rev.* **C52**, 2652 (1995).
[17] A. Dąbrowska, B. Wosiek, C.J. Waddington, *Acta Phys. Pol.* **B31**, 725 (2000).
[18] A. Dąbrowska *et al., Nucl. Phys.* **A693**, 777 (2001).
[19] A.M. Poskanzer, S.A. Voloshin, *Phys. Rev.* **C58**, 1671 (1998).
[20] J.-Y. Ollitrault, *Nucl. Phys.* **A638**, 195c (1998).
[21] A. Dąbrowska *et al., Acta Phys. Pol.* **B32**, 3099 (2001).
[22] P.L. Jain, G. Singh, *Phys. Lett.* **B393**, 193 (1997).
[23] P.L. Jain, *Phys. Lett.* **B366**, 32 (1996).